FEBS Letters 349 (1994) 93–98

FEBS 14265

Crystal structure of the cyanide-inhibited *Xenopus laevis* Cu,Zn superoxide dismutase at 98 K

Kristina Djinovic Carugo[a,*], Andrea Battistoni[b], Maria Teresa Carri[b], Fabio Polticelli[b], Alessandro Desideri[c], Giuseppe Rotilio[b], Alessandro Coda[a], Martino Bolognesi[a,d]

[a]*Dipartimento di Genetica e Microbiologia, Università di Pavia, Via Abbiategrasso 207, 27100 Pavia, Italy*
[b]*Dipartimento di Biologia, Università di Roma 'Tor Vergata', Via della Ricerca Scientifica, 00133 Roma, Italy*
[c]*Dipartimento di Chimica Organica e Biologica, Università di Messina, 98166 Messina, Italy*
[d]*Centro Biotecnologie Avanzate and Dipartimento di Fisica, Università di Genova, Viale Benedetto XV, 16132 Genova, Italy*

Received 23 May 1994; revised version received 15 June 1994

Abstract

The crystal structure of cyanide-inhibited *X. laevis* Cu,Zn superoxide dismutase has been studied and refined based on diffraction data collected at 98 K. The final *R*-factor for the 27,299 reflections in the 10.0–1.7 Å resolution range is 0.170. The cyanide anion, which is a competitive inhibitor expected to mimic the superoxide binding mode, binds directly to the active site copper atom, replacing the coordinated water molecule. Moreover, the anion establishes a strong electrostatic interaction with the guanidinium group of the conserved active site residue Arg^{141}. The coordination sphere of Cu^{2+} is partly altered with respect to the uninhibited enzyme: a displacement of 0.41 Å in subunit A, and 0.27 Å in subunit B of the dimeric enzyme is observed for the Cu^{2+} ions. Only two ligands in the Cu^{2+} coordination sphere (His^{46} and His^{118}) are significantly affected by cyanide binding, whereas virtually no rearrangement of the Zn^{2+} ligands is reported.

Key words: Superoxide dismutase; Cyanide inhibition; Crystal structure

1. Introduction

Cu,Zn superoxide dismutases (SODs) form a very conservative class of enzymes that catalyse the dismutation of the superoxide anion radical (O_2^-) into oxygen and hydrogen peroxide. The overall three-dimensional structure, and in particular the active site region of these enzymes, is highly preserved through evolution [1,2], in agreement with the identical catalytic properties [3] displayed by all the investigated Cu,Zn SODs. The SOD mechanism of action involves two half cycles of reduction and oxidation of the catalytically active copper ion and has been shown to be driven by an asymmetric distribution of the electrostatic potential [4,5], which reaches positive values only in the surroundings of the catalytic site and which is conserved in all the investigated Cu,Zn SOD species [2]. Small monovalent anions are known as inhibitors of Cu,Zn SOD enzymatic activity, and, as shown by investigations on the enzyme–substrate interactions [6], they provide good models for the study of substrate binding modes. In the CN^-, N_3^-, NCO^-, F^-, Cl^- series of small monovalent anions, cyanide has the highest binding constant for Cu,Zn SODs in solution [6,7] ($K_i = 10^5\ M^{-1}$). Moreover, being a diatomic molecule, as is superoxide, it has been considered the best substrate analogue; its interaction with the enzyme has been widely studied by means of spectroscopic techniques, such as solution and single crystal EPR [7,8], Endor [9] spin echo [10], EXAFS [11], and NMR [12,13]. No X-ray structure of the cyanide adduct has so far been reported, although the three-dimensional structure of ox [14], spinach [15], yeast [16] and human [17] Cu,Zn SODs have been solved at a resolution varying between 2.0 and 2.5 Å. Recently the recombinant *Xenopus laevis* Cu,Zn SOD has been crystallised and its structure has been solved to 1.49 Å resolution [18]. The present communication, together with the three-dimensional structure of azide-inhibited bovine Cu,Zn SOD [19], allows the first comparative structural study on SOD–inhibitor recognition in the presence of a di-atomic anion (cyanide) with respect to a three-atomic (azide) anion, and thus a detailed description of the enzyme interaction with substrate analogues.

2. Materials and methods

Orthorhombic crystals of recombinant *X. laevis* Cu,Zn SOD (space group $P2_12_12_1$, one enzyme dimer per asymmetric unit) suitable for X-ray diffraction experiments were grown as described previously [20]. The crystals were soaked for 1 h in a solution containing 0.05 M sodium phosphate, 35% (w/v) PEG4000, 10% (v/v) ethylene glycol, 0.1 M KCN, at pH 7.5, subsequently mounted on a thread loop [21] and shock freezed. The low temperature data collection was required due to the high instability of cyanide-inhibited Cu,Zn SOD crystals in the X-ray beam. Diffraction data were collected at near liquid nitrogen temperature (98(1) K) on a Rigaku RU-200 X-ray generator (λ(CuKα) = 1.54178 Å) using the R-axis II image plate system as detector and Molecular Structure Corp. (The Woodlands, TX, USA) cryo-cooling apparatus. 90,611 intensities were evaluated using the MOSFLM program package [22], and merged into a unique set of 27,299 reflections (85.9% completeness) with the CCP4 program suite [23], to the R_{merge} value of 0.051 for the data in the $\infty - 1.7$ Å resolution range.

* Corresponding author. Fax: (39) (382) 528 496.

SSDI 0014-5793(94)00651-B

As the cell dimensions determined from the data collected at low temperature (a = 72.15, b = 68.10, c = 57.57 Å) were systematically shorter than those measured at 4°C (a = 73.46, b = 68.94, c = 58.76 Å) [18], preliminary rigid body refinement cycles were performed with the TNT program suite [24], starting from the model of the *X. laevis* Cu,Zn SOD refined (R = 0.100) at 1.49 Å resolution. Refinement of individual atomic positional and thermal parameters of the model, without solvent molecules in the active site channel, was subsequently performed, yielding an R-factor of 0.225 for the diffraction data in the 10.0–1.7 Å resolution shell. At this stage a difference electron density map calculated with coefficients $|F_o-F_c|$, and calculated phases, revealed the cyanide anion directly coordinated to the active site copper. The inhibitor atoms were introduced into the model, and the refinement was completed using the PROLSQ program package [25] in combination with the ARP program [26], for automatic location of solvent molecules in the difference electron density maps. During the refinement no restraints were applied to the copper- and zinc-coordination distances. After several rounds of refinement and model/map inspections with FRODO [27], alternative conformations for nine side chains were recognised as indicated from the inspection of the difference Fourier peaks, and introduced in the model.

When the refinement was at convergence, the cyanide atoms were removed from the model, and 20 additional cycles of restrained crystallographic refinement were performed, yielding an R-value of 0.172. A difference electron density map calculated with this omit-model revealed the highest peaks at the sites of bound cyanide anions in both the enzyme subunits of the asymmetric unit, the next difference electron density peak not corresponding to the inhibitor location having 45% lower intensity than these.

3. Results and discussion

The final R-value for 2136 protein atoms, 4 ligand atoms and 498 solvent molecules located in the intermolecular space is 0.170 for the data in the 10.0–1.7 Å resolution range. The average B-factor for the protein atoms is 13.9 Å^2, 11.8 Å^2 for the cyanide atoms, and 30.3 Å^2 for solvent molecules, while the overall temperature factor of the model, including ordered solvent, is 17.0 Å^2. The deviations from the ideal stereochemical parameters are 0.009 Å for bond lengths, 0.016 Å for angle distances, and 0.015 Å for planar 1–4 distances. The estimated coordinates error for the *X. laevis* SOD–cyanide atomic model is 0.15 Å, as determined from the σ_a plot [37]. Inspection of the Ramachandran plot [29] highlights in both monomers residue Asp^{24}, which is located in a β-turn hosting one-residue insertion with respect to the bovine SOD amino acid sequence, as having the $\phi-\psi$ values outside the allowed regions.

When the model of the uninhibited *X. laevis* Cu,Zn SOD (data collected at 4°C) is overlayed with the final model of the cyanide-inhibited enzyme an rms deviation of 0.32 Å for the Cα atoms of the entire dimer is obtained, in agreement with the comparison of structures solved with data collected at widely separated temperatures [28]. A rms displacement of 0.43 Å is observed when all atoms in the two protein dimers are compared.

The cyanide anion, acting as a monodentate ligand, binds to the copper ion through the carbon atom, with coordination distances of 2.20/2.28 Å (subunit A/subunit B); upon cyanide binding the loosely coordinated water molecule observed in the resting enzyme [14–18] is removed. A detailed comparison of the active site geometry of the resting and inhibited SOD forms, as presented in Fig. 1 and Tables 1a and b, shows that the structural rearrangements induced by cyanide binding involve essentially the copper ion itself as well as residues His^{46} and His^{118}. The copper ion is displaced (see Table 1b) from the position occupied in the non-inhibited enzyme similarly to what has been observed in the case of the azide-inhibited bovine Cu,Zn SOD (0.67 Å in subunit A, and 0.37 Å in subunit B [19]). Residue His^{46} moves from a coordination distance typical for a copper(II)–His pair (2.21/2.15 Å in subunit A/subunit B) to significantly longer coordination distances (2.76 Å in subunit A and 2.56 Å in subunit B). On the other hand, a concerted shift of the His^{118} NE2 atom (see Table 1b) maintains, in the case of this residue, the coordination distance to Cu^{2+} almost constant. To a lesser extent His^{61} NE2 atoms in the two subunits also follow the copper movement (see Table 1a,b). Thus, the copper ion is shifted out of the plane defined in the native enzyme by Cu^{2+} and by the coordinating nitrogen atoms of His^{44}, His^{61} and His^{118} residues.

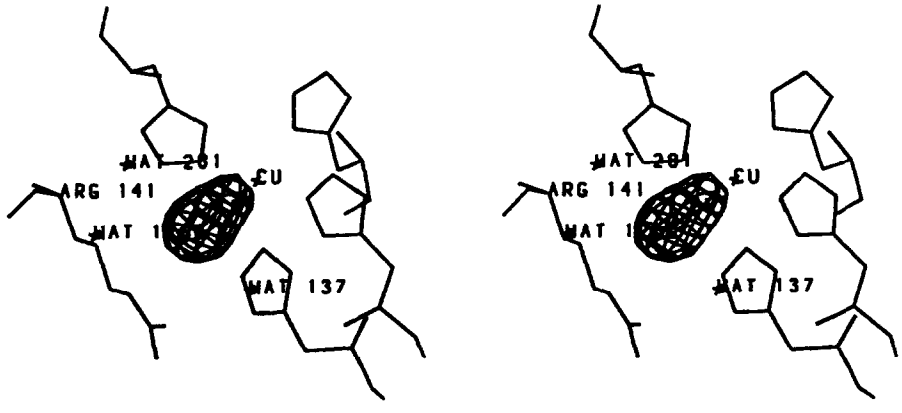

Fig. 1. Stereo drawing of the active site *X. laevis* Cu,Zn SOD together with the bound cyanide anion and the water molecules located in the active site channel, as observed in the inhibited enzyme. The difference electron density for the cyanide anion is contoured at the 3.5 σ level.

The new coordination geometry achieved by the copper ion can be described as distorted square pyramidal: the four base liganding atoms are His^{44} ND1, His^{61} NE2, His^{118} NE2, and the cyanide carbon atom; His^{46} NE2 atom occupies the apical vertex of the coordination polyhedron. These observations are in line with early EPR studies [7] which indicated that in the Cu,Zn SOD–cyanide adduct, the copper coordination is square planar, with the anion lying in a plane together with three histidine imidazole nitrogen atoms. More recent NMR studies on semisynthetic Cu,Co SOD proposed His^{46} as the residue departing from the coordination sphere upon binding of the azide or cyanide inhibitor to the copper ion [30,31].

The distorted tetrahedral coordination geometry of the active site Zn^{2+} ion observed in the uninhibited enzyme is fairly well conserved in the Cu,Zn SOD–cyanide adduct, as can be seen from the contained displacements observed for the zinc ions and for their coordinating ligands (Table 1b). These observations are in line with the interpretation of the EPR data of Cu,Co SOD [32], indicating no change in the Zn^{2+} coordination sphere upon azide binding, as well as with the crystallographic analysis of the bovine Cu,Zn SOD–azide adduct [19].

A strong electrostatic interaction is observed between the bound cyanide anion and Arg^{141}, the distance between cyanide N and the guanidinium NEH2 atoms being 3.31/3.35 Å (subunit A/subunit B). Arg^{141} is considered the most important residue for the electrostatic docking of the superoxide ion in the active site channel [33,34]. Additionally, in subunit A, the cyanide N atom hydrogen bonds to three water molecules, W137, W281 and W126 (2.87, 3.18 and 3.28 Å, respectively) (see Fig. 1). The solvent molecule W137, is at the center of a hydrogen bonded network comprising additional water molecules W371 and W81 (2.43 and 2.89 Å), near the guanidinium group of Arg^{141} residue, and forming a complex scheme of interactions that stabilise the orientation of the inhibitor in the active site channel. In subunit B the cyanide group is hydrogen bonded to three solvent molecules W157, W134 and W431 (2.68, 3.15 and 3.35 Å) which are arranged similarly to W137, W280 and W126 in subunit A. On the other hand, the solvent molecule closest to the cyanide anion, W157, does not build up a hydrogen bonding scheme with Arg^{141} comparable with that of subunit A, due to the crystal lattice contact of the Arg^{141} guanidinium group with the carboxylate of residue Glu^{88} from a symmetry-related SOD molecule (2.91 Å) (Fig. 2). Residue Glu^{88} acts as a polar bridge between the Arg^{141} guanidinium group and the solvent molecule (W157) bound to the inhibitor.

Comparison of the copper coordination spheres of azide-inhibited bovine Cu,Zn SOD and cyanide-inhibited *X. laevis* Cu,Zn SOD (Fig. 3) shows that the pertur-

Table 1a
Coordination distances (in Å) for the Cu^{2+} and Zn^{2+} centers in the A and B subunits of *X. laevis* Cu,Zn SOD–cyanide complex, of the uninhibited *X. laevis* enzyme [16], and of the bovine Cu,Zn SOD–azide complex [17]

	Cu,Zn SOD–cyanide		Cu,Zn SOD		bovine Cu,Zn SOD–azide	
	A	B	A	B	A	B
Cu^{2+}						
His^{44} ND1	2.20	2.13	2.02	1.98	2.05	2.05
His^{46} NE2	2.76	2.56	2.21	2.15	2.65	2.75
His^{61} NE2	2.15	2.12	2.06	2.07	2.18	2.07
His^{118} NE2	2.30	2.24	2.08	2.09	2.01	2.23
Inhibitor/water	2.20	2.28	2.23	2.42	1.97	2.18
Zn^{2+}						
His^{61} ND1	1.94	1.98	2.05	2.02	2.01	2.07
His^{69} ND1	2.28	2.13	2.04	2.02	2.10	2.08
His^{78} ND1	2.19	2.12	2.08	2.05	2.09	1.87
Asp^{81} OD1	1.95	1.94	2.02	1.96	1.84	1.90

Table 1b
Table Positional displacements (in Å) of the metals and metal liganding atoms upon cyanide binding to Cu,Zn SOD

	A	B		A	B
Cu^{2+}	0.41	0.27	Zn^{2+}	0.20	0.19
His^{44} ND1	0.16	0.11	His^{61} ND1	0.06	0.11
His^{46} NE2	0.52	0.45	His^{69} ND1	0.24	0.19
His^{61} NE2	0.32	0.15	His^{78} ND1	0.19	0.17
His^{118} NE2	0.42	0.33	Asp^{81} OD1	0.13	0.19

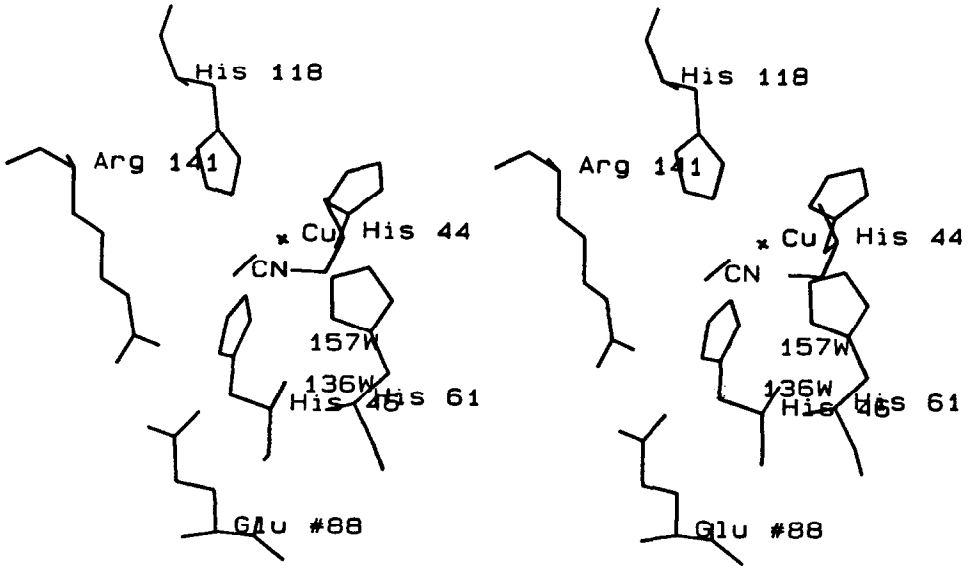

Fig. 2. Stereo drawing of the active site of cyanide-inhibited Cu,Zn SOD monomer B, showing the side chain of the symmetry-related residue Glu^{88} forming an electrostaic interaction with Arg^{141} and hydrogen bonded with solvent molecules 157WAT and 136WAT.

bations occurring upon anion binding bring about very similar active site structures. These structural perturbations can be summarised as contained overall increases of all coordination distances from Cu^{2+} (see Table 1a). In contrast, analysis of the X-ray absorption spectra [11] suggests that the copper–imidazole coordination distances shorten to 1.95(3) Å in the Cu,Zn SOD–cyanide adduct, due to the increase in ligand field strength resulting from cyanide binding; in this context, however, we noticed that these experiments systematically report shorter metal–ligand coordination distances with respect to the crystallographic data even in the case of the resting enzyme [11]. Such a disagreement could possibly be related to the restraining models used to fit the spectroscopic data or to the largely different physicochemical conditions of the two experiments.

The main structural difference between the Cu,Zn SOD–cyanide and –azide complexes can be noticed in the spatial orientation of the bound anion. In the Cu,Zn SOD–azide complex, the linear anion is orientated along the active site channel, while in the case of cyanide it is rotated by approximately 50° towards the Arg^{141} guanidinium group (see Fig. 3). As a result, the interactions between the coordinated anion and the guanidinium

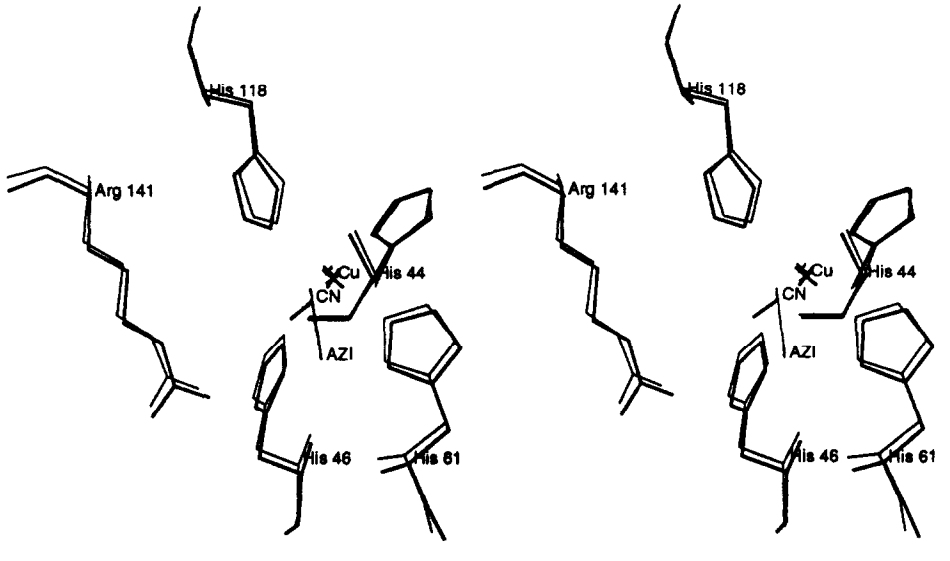

Fig. 3. Stereo drawing of the active site of cyanide-inhibited Cu,Zn SOD (bold line) and azide-inhibited bovine Cu,Zn SOD (thin line) along with the bound inhibitors and the solvent molecules.

group of Arg^{141} are significantly altered. The ligand N...Arg^{141} NEH2 distance (3.31/3.35 Å in subunits A/B of the Cu,Zn SOD–cyanide complex) increases to 3.61/3.67 Å in the Cu,Zn SOD–azide complex [19]. If the azide anion is forced in the same orientation observed for cyanide, severe intramolecular contacts occur with the Arg^{141} side chain, highlighting the finely tuned design of the Cu,Zn SOD active site for a di-atomic substrate. This observation may explain the slower ligand exchange dynamics between free and complexed enzymes observed by NMR, in the case of the Cu,Zn SOD–cyanide with respect to the –azide complexes [12].

The higher SOD affinity for cyanide, with respect to azide [6,7], can therefore be explained not only on the basis of electronic configuration and coordination chemistry of the ligand–metal system, but, in part, also on the mechanistic base of substrate docking in the active site, achieving different levels of interaction with the surrounding structure. A key role in the Cu,Zn SOD–cyanide adduct, in this context, is played by water molecules W137 and W157 (in subunit A and B, respectively), which are strongly hydrogen bonded to the di-atomic ligand, and interestingly, are located approximately at the positions of the free-end inhibitor N atoms in the Cu,Zn SOD–azide complex (Fig. 3). The different accessibility of the active site channels for the two SOD subunits in the crystalline environment is reflected by the higher temperature factors of the cyanide anion in subunit B (14.28 $Å^2$) with respect to subunit A (9.29 $Å^2$), possibly indicating a slightly lower ligand occupancy or limited conformational disorder at site B.

The average temperature factors for the copper liganding atoms (including cyanide, for subunits A/B) are 11.15/12.12 $Å^2$, well below the mean value of the model thermal parameters (17.0 $Å^2$). The lowest thermal parameter is observed for the His^{46} NE2 atom in both subunits, despite the displacement of about 0.5 Å of this residue upon cyanide binding (see Table 1b). On the other hand, the Debye-Waller factors of both the copper ions are above the mean value of the whole model (18.53/18.74 $Å^2$, for subunits A/B, respectively) whereas the zinc cations do not show such a behaviour (10.53/10.94 $Å^2$).

As a whole the results here reported show that contained but definite structural perturbations of the Cu^{2+} coordination sphere occur upon cyanide binding. Despite the observed differences in the inhibitors' binding mode, the tri-atomic azide anion has been shown to affect the copper coordination sphere in a comparable way with respect to the substrate-simulating di-atomic cyanide [19]. The contained rearrangements of the copper catalytic site are a prerequisite for the fast turnover rates measured for the Cu,Zn SODs [35], which must be based on rapid readjustments in the Cu^{2+} ligands. On the other hand, the pronounced mobility of the copper ion, even at the liquid nitrogen temperature, could be attributed to dynamic or static Jahn-Teller distortion of copper [36]. In terms of the enzymatic activity, such structural behaviour might be necessary for the effective accomplishment of the catalytic cycle.

Acknowledgements: This work has been supported by grants from the EC program 'Human Capital and Mobility' and from the CNR Target Oriented Project 'Biotecnologie e Biostrumentazione', from the Ministry of University and Scientific Research of Italy and from Centro Interuniversitario Studio Macromolecole Informazionali.

References

[1] Bordo, D., Djinovic, K. and Bolognesi, M. (1994) J. Mol. Biol. (in press).
[2] Desideri, A., Falconi, M., Polticelli, F., Bolognesi, M., Djinovic, K. and Rotilio, G. (1992) J. Mol. Biol. 223, 337–342.
[3] O'Neill, P., Davies, S., Calabrese, L., Capo, C., Marmocchi, F., Natoli, G. and Rotilio, G. (1988) J. 251, 41–46.
[4] Klapper, I., Hagstrom, R., Fine, R., Sharp, K. and Honig, B. (1986) Proteins 1, 47–59.
[5] Getzoff, E.D., Tainer, J.A., Stempien, M.M., Bell, G.I. and Hallewell, R.A. (1989) Proteins 5, 322–336.
[6] Rigo, A., Stevenato, R., Viglino, P. and Rotilio, G. (1977) Biophys. Res. Commun. 79, 776–783.
[7] Rotilio, G., Morpurgo, L., Giovagnoli, C., Calabrese, L. and Mondovi, B. (1972) Biochemistry 11, 2187–2192.
[8] Lieberman, R.A., Sands, R.H. and Fee, J.A. (1982) J. Biol. Chem. 257, 336–344.
[9] Van Camp, H.L., Sands, R.H. and Fee, J.A. (1982) Biochim. Biophys. Acta 704, 75–89.
[10] Fee, J.A., Peisach, J. and Mims, W.B. (1981) J. Biol. Chem. 256, 1910–1914.
[11] Blackburn, N.J., Strange, R.W., McFadden, L.M. and Hasnain, S.S. (1987) J. Am. Chem. Soc. 109, 7162–7170.
[12] Paci, M., Desideri, A. and Rotilio, G. (1988) J. Biol. Chem. 263, 162–166.
[13] Bertini, I., Lanini, G., Luchinat, L., Messori, L., Monnannini, R. and Scozzafava, A. (1985) J. Am. Chem. Soc. 107, 4391–4396.
[14] Tainer, J.A., Getzoff, E.D., Beem, K.M., Richardson, J.S. and Richardson, D.C. (1982) J. Mol. Biol. 160, 181–217.
[15] Kitagawa, Y., Tanaka, N., Hata, Y., Kusonoki, M., Lee, G., Katsube, Y., Asada., K., Aibara, S. and Morita, Y. (1991) J. Biochem. 109, 447–485.
[16] Djinovic, K., Gatti, G., Coda, A., Antolini, L., Pelosi, G., Desideri, A., Falconi, M., Marmocchi, F., Rotilio, G. and Bolognesi, M. (1992) J. Mol. Biol. 225, 791–809.
[17] Parge, H.E., Hallewell, R.A. and Tainer, J.A. (1992) Proc. Natl. Acad. Sci. USA, 89, 6109–6113.
[18] Djinovic Carugo, K., manuscript in preparation.
[19] Djinovic Carugo, K., Polticelli, F., Desideri, A., Rotilio, G., Wilson, K. S. and Bolognesi, M. (1994) J. Mol. Biol. (in press).
[20] Djinovic Carugo, K., Collyer, C., Coda, A., Carri, M.T., Battistoni, A., Bottaro, G., Polticelli, F., Desideri, A. and Bolognesi, M. (1993) Biochem. Biophys. Res. Commun. 194, 1008–1011.
[21] Teng, T. (1990) J. Appl. Cryst. 23, 387–391.
[22] Leslie, A.G.W. (1991) Daresbury Lab. Inf. Q. Prog. Crystallogr. 26 (available from the Librarian, SERC Laboratory, Daresbury, Warrington, WA4 4AD, UK).
[23] CCP4 (1979) The SERC (UK) Collaborative Computing Project No. 4, a Suite pof Programs for Protein Crystallography, distributed from Daresbury Laboratory, Warrington, WA 4AD, UK.
[24] Tronrud, D.E., TenEyck, L.F. and Matthews, B.W. (1987) Acta Cryst. A43, 489–501.

[25] Konnert, J.H. and Henderickson, W.A. (1980) Acta Cryst. A36, 344–350.
[26] Lamzin, V.S. and Wilson, K.S. (1993) Acta Cryst. D49, 129–147.
[27] Jones, T.A. (1978) J. Appl. Cryst. 11, 268–272.
[28] Tilton Jr., R.F., Dewan, J.C. and Petsko, G.A. (1992) Biochemistry 31, 2469–2481.
[29] Ramakrishnan, C. and Ramachandran, G.N. (1965) Biophys. J. 5, 909–933.
[30] Banci, L., Bertini, I., Luchinat, C. and Scozzafava, A. (1989) J. Biol. Chem. 264, 9742–9744.
[31] Banci, L., Bencini, A., Bertini, I., Luchinat, C. and Piccioli, M. (1990) Inorg. Chem. 29, 4867–4873.
[32] Rotilio, G., Calabrese, L., Mondovi, B. and Blumberg, W.E. (1974) J. Biol. Chem. 249, 3157–3160.
[33] Tainer, J.A., Getzoff, K.M., Richardson, J.S. and Richardson, D.C. (1983) Nature, 306, 284–287.
[34] Osman, R. (1986) Enzyme 36, 32–43.
[35] McAdam, M., Fielden, E.M., Lavelle, F., Calabrese, L., Cocco, D. and Rotilio, G. (1977) Biochem. J. 167, 271–274.
[36] Hathaway, B.J. (1984) Structure Bonding 57, 55–118.
[37] Read, R.J. (1986) Acta Cryst. A42, 140–149.